JOURNAL OF BACTERIOLOGY, Oct. 2010, p. 4935–4943 Vol. 192, No. 19
0021-9193/10/$12.00 doi:10.1128/JB.00614-10

A Novel Replicative Enzyme Encoded by the Linear *Arthrobacter* Plasmid pAL1▽†

Stephan Kolkenbrock,[1]‡ Bianca Naumann,[2] Michael Hippler,[2] and Susanne Fetzner[1]*

Institute of Molecular Microbiology and Biotechnology[1] and Institute of Plant Biochemistry and Biotechnology,[2] Westfalian Wilhelms-University Münster, Münster, Germany

Received 30 May 2010/Accepted 25 July 2010

The soil bacterium *Arthrobacter nitroguajacolicus* Rü61a contains the linear plasmid pAL1, which codes for the degradation of 2-methylquinoline. Like other linear replicons of actinomycetes, pAL1 is characterized by short terminal inverted-repeat sequences and terminal proteins (TP_{pAL1}) covalently attached to its 5′ ends. TP_{pAL1}, encoded by the *pAL1.102* gene, interacts *in vivo* with the protein encoded by *pAL1.101*. Bioinformatic analysis of the pAL1.101 protein, which comprises 1,707 amino acids, suggested putative zinc finger and topoisomerase-primase domains and part of a superfamily 2 helicase domain in its N-terminal and central regions, respectively. Sequence motifs characteristic of the polymerization domain of family B DNA polymerases are partially conserved in a C-terminal segment. The purified recombinant protein catalyzed the deoxycytidylation of TP_{pAL1} in the presence of single-stranded DNA templates comprising the 3′-terminal sequence (5′-GCAGG-3′), which in pAL1 forms the terminal inverted repeat, but also at templates with 5′-(G/T)CA(GG/GC/CG)-3′ ends. Enzyme assays suggested that the protein exhibits DNA topoisomerase, DNA helicase, and DNA- and protein-primed DNA polymerase activities. The pAL1.101 protein, therefore, may act as a replicase of pAL1.

Linear plasmids have been identified in higher plants, fungi, and many bacteria. Most of these linear genetic elements are characterized by terminal inverted-repeat sequences and terminal proteins (TPs) covalently attached to their 5′ ends. The presence of TPs is a consequence of their mode of DNA replication, which in linear plasmids of plants, yeasts, and fungi is initiated at the termini by using the TP as a primer and proceeds by strand displacement. The DNA polymerases encoded by these linear elements are of the viral B type, related to those of contemporary adenoviruses and *Bacillus* phages (29). The mechanism of protein-primed DNA replication has been studied in detail, especially for the model of *Bacillus subtilis* phage ϕ29, which uses a monomeric B-family DNA polymerase for both the TP-primed initiation reaction and DNA elongation, resulting in continuous, full-length replication of both strands of the ϕ29 genome (5, 6, 7, 26, 42, 43, 44). In contrast to the linear plasmids of eukaryotes, linear chromosomes and plasmids of *Streptomyces* spp. replicate bidirectionally from an internal origin (9). This replication mechanism encounters the problem that discontinuous lagging-strand synthesis from RNA-primed Okazaki fragments leaves recessed 5′ ends at both telomeres when the distal RNA primers are removed. In the *Streptomyces* linear replicons, the TP serves as a primer for filling in these single-stranded gaps (2, 58). Both the TP and a telomere-associated protein (Tap), which is presumed to recruit the TP and position it at the telomere, are necessary for the propagation of *Streptomyces* replicons in their linear forms (3).

The TP and the Tap protein are highly conserved among many *Streptomyces* species. On the other hand, several studies have suggested a considerable diversity of streptomycetal replication systems. Replication in linear form of the plasmid pRL2 of *Streptomyces* sp. strain 44414, for example, requires the *pRL2.3c* and *pRL2.4* genes, coding for a putative TP and a presumed Tap-helicase protein, respectively (59, 60). The linear chromosome of *Streptomyces griseus* IFO13350 also has an unusual telomere-associated protein, which has a DnaB-like helicase C-terminal domain (54). The linear plasmid SCP1 of *Streptomyces coelicolor* A3(2) requires the *SCP1.127* gene, coding for a unique TP, and *SCP1.125* for replication of its telomeres (24, 52). Linear plasmids also occur in other actinomycetes besides the streptomycetes, e.g., in several members of the rhodococci and mycobacteria, but their replicative proteins have not been studied yet.

The genus *Arthrobacter* has been classified in the family *Micrococcaceae* within the order *Actinomycetales*. The 113-kb conjugative plasmid pAL1, which confers on *Arthrobacter nitroguajacolicus* Rü61a the ability to utilize the N-heteroaromatic compound 2-methylquinoline, is so far the only described linear plasmid within this genus. The termini of pAL1 show the inverted-repeat sequence 5′-CCTGC…GCAGG-3′, and its 5′ ends are capped with proteins (34, 36). The terminal protein TP_{pAL1} is encoded by the *pAL1.102* locus, which is located close to the "right" terminus of pAL1 (30). The adjacent gene *pAL1.101* codes for a putative telomere-associated protein, which, however, is much larger than the Tap proteins of *Streptomyces* linear replicons. We hypothesized that the pAL1.101 protein might play a different, or more versatile, role

* Corresponding author. Mailing address: Institute of Molecular Microbiology and Biotechnology, Westfalian Wilhelms-University Münster, Corrensstrasse 3, D-48149 Münster, Germany. Phone: 49 251 83 39824. Fax: 49 251 83 38388. E-mail: fetzner@uni-muenster.de.

‡ Present address: Institute of Plant Biochemistry and Biotechnology, Westfalian Wilhelms-University Münster, D-48143 Münster, Germany.

† Supplemental material for this article may be found at http://jb.asm.org/.

▽ Published ahead of print on 30 July 2010.

in the replication of linear DNA than the Tap proteins (36). In this study, we show that the protein interacts with TP_{pAL1} *in vivo*. As a precondition for biochemical studies, we established a protocol for the preparation of recombinant pAL1.101 protein. The first data on its catalytic properties suggest that it exhibits DNA topoisomerase, DNA helicase, and DNA- and TP-primed DNA polymerase activities. It thus can be considered a novel replicative enzyme, which we have named REP_{pAL1}.

MATERIALS AND METHODS

Bacterial strains, media, and growth conditions. The strains and plasmids used in this study are listed in Table S1 in the supplemental material. For isolation of total DNA, *A. nitroguajacolicus* Rü61a(pAL1) was grown in mineral salts medium (35) on 8 mM sodium benzoate at 30°C. For the preparation of crude extract supernatant for use in the deoxycytidylation assay, *A. nitroguajacolicus* Rü61a(pAL1) was grown in lysogeny broth (LB) (45). *A. nitroguajacolicus* Rü61a(pAL1, pART2-ORF102) was grown in mineral salts medium on 4 mM 4-hydroxyquinaldine in the presence of 140 μg/ml kanamycin. *E. coli* clones containing derivatives of pART2 or pET-22b(+) were grown in LB with 50 μg/ml kanamycin or 100 μg/ml ampicillin, respectively, at 37°C. For synthesis of maltose binding protein (MBP) and REP_{pAL1} fusion protein, *Escherichia coli* Rosetta 2(DE3)(pLysSRARE2) harboring either pET22b-*malE*-his_6 or pET22b-ORF101 was grown in LB with ampicillin (100 μg/ml), chloramphenicol (34 μg/ml), and autoinduction solutions 5052 and M (53) at 30°C. Cells were harvested by centrifugation and stored at −80°C prior to use.

DNA techniques. Total DNA of *A. nitroguajacolicus* Rü61a(pAL1) was isolated according to the method of Rainey et al. (39). Plasmid DNA was isolated with the E.Z.N.A. Plasmid Miniprep kit (peqlab, Erlangen, Germany). Gel extraction of DNA fragments from agarose gels was performed with the Perfectprep gel cleanup kit (Eppendorf, Hamburg, Germany). For cloning purposes, DNA fragments were purified with the High Pure PCR Product Purification kit (Roche Diagnostics GmbH, Mannheim, Germany). Standard protocols were used for agarose gel electrophoresis, restriction digestion, and DNA ligation (45). ORF101 of pAL1 was amplified by PCR with Phusion Hot Start High-Fidelity DNA Polymerase (Finnzymes Oy, Espoo, Finland), using total DNA of *A. nitroguajacolicus* Rü61a(pAL1) as the template. The primers and all oligonucleotides used are listed in Table S2 in the supplemental material. Competent *E. coli* and *A. nitroguajacolicus* Rü61a(pAL1) cells were generated as described in references 22 and 17, respectively. Plasmid inserts and flanking regions were verified by sequencing. Southern transfer of DNA from polyacrylamide gels to nylon membranes (Parablot NY plus; Macherey-Nagel, Dülmen, Germany) was done by capillary blotting. Colorimetric immunodetection of digoxigenin (DIG)-labeled DNA was performed using Anti-DIG-AP (Fab fragments from anti-digoxigenin antibody conjugated with alkaline phosphatase), nitroblue tetrazolium chloride, and 5-bromo-4-chloro-3-indolyl phosphate as described previously (40).

Protein purification. The TP_{pAL1} protein with an N-terminal fusion to MBP was purified from *E. coli* ER2508(pLysSRARE, pMal-c2x-ORF102) as described previously (30). REP_{pAL1} protein was isolated with an N-terminal MBP-His_7 and a C-terminal His_6 fusion from *E. coli* Rosetta 2(DE3)(pLysSRARE2, pET22b-ORF101). Cell suspensions in 20 mM Tris-HCl buffer (pH 7.4) containing 400 mM NaCl, 1 mM EDTA, 1 mM phenylmethylsulfonyl fluoride, 1 M NDSB-201 [3-(1-pyridino)-1-propanesulfonate], 1 mM $MgCl_2$, and 10 U/ml of benzonase were incubated for 30 min at room temperature and sonicated briefly, and crude extract supernatant was obtained by centrifugation. The crude extract (50 ml, from 20 g wet biomass) was applied to an amylose column (5 ml), which was then washed with 20 mM Tris-HCl buffer (pH 7.4) containing 400 mM NaCl and 1 mM EDTA. REP_{pAL1} was eluted with 20 mM maltose dissolved in the same buffer supplemented with 200 mM NDSB-201. Subsequently, the protein was subjected to size exclusion chromatography on a HiLoad 26/60 Superdex 200 column (GE Healthcare, Munich, Germany) in 20 mM Tris-HCl (pH 7.4; 400 mM NaCl, 1 mM EDTA). The pooled fractions were mixed with NDSB-201 to a concentration of 200 mM and concentrated in a U-Tube concentrator 15H-30 (Novagen).

For control experiments, MBP-His_6 protein was prepared from *E. coli* Rosetta 2(DE3)(pLysSRARE2, pET22b-malE-His_6)—i.e., from an *E. coli* strain that, apart from the *pAL1.101* gene, is isogenic to the clone used for isolation of the REP_{pAL1} fusion protein—by the same amylose affinity chromatography protocol as that applied for the first step of REP_{pAL1} purification.

Protein concentrations were determined by the bicinchoninic acid method (48). Proteins separated in SDS-polyacrylamide gels were stained with ethyl violet and zincon (10).

***In vivo* formaldehyde cross-linking and identification of proteins cross-linked with TP_{pAL1}.** Cell suspensions of *A. nitroguajacolicus* Rü61a(pAL1, pART2-ORF102), washed in phosphate-buffered saline (pH 7.4) and adjusted to an optical density at 600 nm (OD_{600}) of 10, were incubated in 0%, 0.2%, and 0.5% (by volume) formaldehyde for 30 min at 22°C. The reaction was stopped by addition of glycine (0.125 M), the cells were washed in phosphate-buffered saline, resuspended in denaturing buffer (50 mM sodium phosphate buffer, pH 8.0, 300 mM NaCl, 1% [wt/vol] SDS), and disrupted by sonication. Cell extracts were incubated with Ni^{2+}-nitrilotriacetate (NTA) agarose beads for 10 min at room temperature. Beads with adsorbed proteins were recovered by centrifugation using Spin Columns (Perfectprep; Eppendorf, Hamburg, Germany) and washed with 50 mM phosphate buffer, 300 mM NaCl, pH 8. The bound protein complexes were eluted with phosphate buffer adjusted to pH 5.5, concentrated, and separated in SDS-polyacrylamide gels (10.8% acrylamide; Coomassie stain). Protein bands that, according to immunodetection on a corresponding Western blot (anti-His_5 antibody), contained covalent complexes with TP_{pAL1}-His_8 were excised from the polyacrylamide gel. In-gel tryptic digestion was performed according to the method of Stauber et al. (49). Liquid chromatography-tandem mass spectrometry (LC-MS/MS) analyses were conducted as described previously (50), using an Ultimate 3000 nano-liquid chromatography system (Dionex, Sunnyvale, CA) and an LTQ Orbitrap XL (Thermo, Bremen, Germany) mass spectrometer. The measured MS/MS spectra were matched with tryptic amino acid sequences deduced from all six reading frames of pAL1 (GenBank accession no. AM286278.2) and to those deduced from the genome of *Arthrobacter aurescens* TC1 (CP000474) using SEQUEST as previously described (49).

DNA relaxation assay. In all assays for catalytic activities of REP_{pAL1}, 35 mM Tris-HCl, 72 mM KCl, 5 mM dithiothreitol, 5 mM $MgCl_2$ (pH 8) was used as a basal buffer. For the detection of DNA relaxation activity of REP_{pAL1}, pET-22b(+) plasmid DNA was incubated with the purified protein in the presence or absence of $MgCl_2$. Aliquots withdrawn at appropriate time intervals were quenched in liquid N_2 and subsequently separated in an agarose gel. DNA topoisomerase I from calf thymus (Takara Bio Europe); the site- and strand-specific endonuclease Nt.Bpu10I (Fermentas GmbH, St.Leon-Rot, Germany), which creates a single nick in pET-22b(+); and the restriction endonuclease HindIII to generate linearized plasmid DNA were used for control assays. The DNA forms generated were separated in agarose gels. By adding 1 μg/ml ethidium bromide to the gel buffer, it was possible to separate relaxed covalently closed circular DNA, as generated by topoisomerase I, from other DNA forms (11).

Helicase assays. The 5′-DIG labeled 29-mer oligonucleotide DIG29basic, hybridized to either (i) the fully complementary oligomer blunt29; (ii) the 29-mer 29-3, generating 6-nucleotide 3′ overhangs; or (iii) the 29-mer 29-5, generating 6-nucleotide 5′ overhangs, was used as a DNA substrate for a strand displacement assay (for the oligonucleotide sequences, see Table S2 in the supplemental material). Hybridization of DIG29basic (33 μM) and the respective unlabeled complementary oligonucleotide (66 μM) was performed in a thermocycler using a stepwise gradient from 98°C (10 min) through 80°C (2 min), 73°C (10 min), and 70°C, 65°C, 60°C, 50°C, 40°C, and 30°C (2 min each) to 20°C. Hybridized double-stranded DNA (dsDNA) substrates, after dilution in H_2O, were mixed with a 100-fold excess of unlabeled competitor DNA, which in the case of complete unwinding of the dsDNA, mediated by helicase activity of REP_{pAL1}, outcompetes rehybridization of DIG29basic and thus releases the labeled 29-mer as single-stranded DNA (ssDNA). The respective dsDNA substrate, competitor DNA, and REP_{pAL1} protein (or MBP-His_6 in control samples) were incubated in the presence or absence of ATP or dATP, separated in a polyacrylamide gel, and transferred by Southern blotting to a nylon membrane. Colorimetric detection of DIG-labeled fragments was performed with anti-DIG-AP antibodies (Fab fragments conjugated with alkaline phosphatase; Roche), *p*-nitrotetrazolium blue, and 5-bromo-4-chloro-3-indolyl phosphate. Helicase activity was also measured in a continuous fluorometric assay, which was based on the displacement of the fluorescent dye DAPI (4′,6-diamidino-2-phenylindole) from dsDNA upon DNA unwinding (16). pUC18 DNA, linearized with HindIII, PstI, or SmaI, was used as a substrate. To test 5′-capped dsDNA as a potential substrate, an ~3-kb stretch of DNA was amplified using pET-22b(+) as a template and 5′-biotinylated primers (see Table S2 in the supplemental material), and the amplicon was purified from an agarose gel. Fluorescence measurements were performed in a Jasco FP-6500 spectrofluorimeter, using excitation and emission wavelengths of 345 and 467 nm and bandwidths of 1 and 10 nm for the excitation and emission splits, respectively. The value for 100% unwinding was obtained by subtracting the fluorescence of an equimolar amount of ssDNA (dsDNA substrate dena-

tured at 98°C and quenched in liquid N_2) (F_{ssDNA}) from the initial fluorescence of dsDNA (F_{dsDNA}). These values were determined for each set of reaction conditions and each DNA substrate tested. The observed fluorescence change (F_{obs}) divided by ($F_{dsDNA} - F_{ssDNA}$) indicates the extent of unwinding. Initial unwinding rates were estimated from the initial slopes of the kinetic traces. The percentage of total DNA unwound was multiplied by the concentration of base pairs in the reaction mixture, and the total concentration of unwound base pairs was divided by the time required for complete unwinding to estimate the apparent rate (16, 41).

Deoxycytidylation of TP_{pAL1}. The template specificity of REP_{pAL1}-catalyzed deoxycytidylation of TP_{pAL1} was analyzed in an *in vitro* assay as described previously (30).

DNA polymerase assays. Protein-primed DNA amplification by REP_{pAL1} was analyzed using the 285-bp dsDNA template l285 (see Table S2 in the supplemental material) with purified MBP-TP_{pAL1} as a primer. The product was treated with proteinase K prior to agarose gel electrophoresis. The ability of REP_{pAL1} to elongate a DNA primer-template hybrid was tested with the left50/left13t hybrid molecule (see Table S2 in the supplemental material). Annealing of the two oligomers was performed in a thermocycler using a stepwise gradient from 98°C (2 min) through 65°C (2 min), 55°C (10 min), and 50°C, 40°C, and 30°C (2 min each) to 10°C. The hybrid DNA was incubated with dATP, dGTP, dTTP, dithiothreitol, [α-^{32}P]dCTP, and purified REP_{pAL1} protein; controls were performed with MBP-His_6 instead of REP_{pAL1}. The reaction products were analyzed in a 15% polyacrylamide gel.

RESULTS

REP_{pAL1} is a multidomain protein. REP_{pAL1}, the product of the *pAL1.101* gene, comprises 1,707 amino acids (aa) and has a predicted molecular mass of ~186.8 kDa. In its C-terminal region, it shows sequence similarity to part of the Tap proteins of *Streptomycetes*, e.g., 29% identity of aa 1446 to 1663 of REP_{pAL1} to aa 415 to 678 of TapL of *Streptomyces lividans*. Closer homologs of REP_{pAL1} occur in the genus *Rhodococcus*. Several gene products of comparable size, encoded by rhodococcal linear plasmids, exhibit >30% overall identity to REP_{pAL1}. Examples are the pROB01-00090 protein of *Rhodococcus opacus* B4 and the pREL1_00080 protein of *Rhodococcus erythropolis* strain PR4, which have been annotated as putative telomere-binding proteins, and the protein encoded by the RHA1_ro10009 locus of pRHL2 of *Rhodococcus jostii* RHA1.

A search for conserved domains in REP_{pAL1} revealed similarity of its N-terminal region to DnaG-type proteins; this region includes fully conserved CHC2-type zinc finger and topoisomerase-primase (Toprim) domains (Fig. 1A). The consensus of a "zinc ribbon" (19), as well as the EGXXD and DXD motifs, which in Toprim-containing enzymes are involved in coordination of Mg^{2+} and catalysis (1, 47), are conserved in REP_{pAL1}, as well as in its rhodococcal orthologs. Residue Y469 of REP_{pAL1} is also strictly conserved among the related rhodococcal proteins. A centrally located region (aa 598 to 868), which contains Walker A- and Walker B-like motifs potentially involved in nucleotide binding, aligns with part of the COG5519 domain of superfamily 2 helicases (Fig. 1A). Besides the Walker A and B boxes (56), which are conserved in all helicases, residues ^{809}MGITGS^{814} of REP_{pAL1} might correspond to motif III (+X+TGS, where + is hydrophobic and X is any amino acid) of helicase superfamily 2 (20); however, due to the substantial divergence of motif sequences, it is difficult to predict helicase motifs solely from an amino acid sequence (8). Further downstream in the REP_{pAL1} sequence, a CXXC$(X)_{13-14}$HXXC motif at positions 1155 to 1175 that is also conserved in the rhodococcal homologs might form a binding site for divalent metal ions.

There was no significant similarity to known conserved domains in the large C-terminal region of REP_{pAL1}, and it was not feasible to predict putative function from sequence analysis. However, alignments tentatively suggested partial conservation of motifs A (DX_2SLYP) and B (KX_3NSXYG), which are characteristic of the polymerization domain of family B DNA polymerases (Fig. 1B). Residues of these motifs contribute to the polymerization active site and are involved in binding of metal ions (Asp of motif A) and binding of deoxynucleoside triphosphates (dNTPs) (Tyr residues of motifs A and B) (7). Notably, motif A- and motif B-like sequences seem to be absent in TapL of *Streptomyces* (Fig. 1B). A region reminiscent of the so-called TPR-1 sequence ([R/K][X]$_{6-10}$[Y/W/F][X]$_{12-16}$[D/E][L/I/W][X]$_{6-8}$[Y/W/F]X[L/I/V/F][X]$_{7-14}$[F/W/Y]), located between motifs A and B of protein-priming DNA polymerases, might be conserved in both REP_{pAL1} (^{1507}K[X]$_{26}$L[X]$_7$YEL[X]$_7$W^{1552}) and TapL (Fig. 1B). In phage ϕ29 DNA polymerase, TPR-1 was demonstrated to be important for positioning of the protein primer and for transition between protein-primed and DNA-primed modes of replication (14, 15, 27, 37). A sequence corresponding to motif C of DNA polymerases (YX DTDS), which via its Asp residues contributes to metal ion binding and catalysis (7), was not obvious in REP_{pAL1}. However, in a C-terminal region that is highly conserved among REP_{pAL1} and its rhodococcal homologs, a number of acidic residues are conserved (Fig. 1C), some of which might be involved in the two-metal-ion mechanism of DNA polymerases (51). Despite only distant relatedness to known proteins, sequence analysis suggested that REP_{pAL1} might act as a multifunctional enzyme in DNA replication; however, the functional significance of individual domains and of conserved amino acid residues remains to be investigated.

REP_{pAL1} interacts *in vivo* with the terminal protein TP_{pAL1}. To address the question of whether REP_{pAL1}, together with the terminal protein TP_{pAL1}, is part of a telomeric complex, octahistidine-tagged TP_{pAL1} was synthesized in the homologous host, and interacting proteins were captured by *in vivo* cross-linking. From cells of *A. nitroguajacolicus* Rü61a(pAL1, pART2-ORF102) treated with formaldehyde, the covalent complex of TP_{pAL1}-His_8 was prepared by denaturing metal chelate affinity chromatography and gel electrophoresis and subjected to trypsin digestion, and peptides were identified by LC-MS/MS analysis (see Table S3 in the supplemental material). The complex from cells treated with 0.5% formaldehyde contained fragments of TP_{pAL1}, as well as peptides that were assigned to proteins which probably were highly expressed in the cytoplasm, such as superoxide dismutase, encoded by *pAL1.014*, and a predicted GroEL protein. In the tryptic digest of the protein complex purified from cells soaked in 0.2% formaldehyde, fragments of TP_{pAL1} (aa 34 to 49, 145 to 168, 169 to 181, and 182 to 192) and of the N-terminal region of REP_{pAL1} (Fig. 1A) exclusively were identified, suggesting specific interaction of these proteins *in vivo*.

Preparation of REP_{pAL1} fusion protein. The *pAL1.101* gene was expressed in *E. coli* cotransformed with a plasmid carrying tRNA genes for codons rarely used in *E. coli* (see Table S1 in the supplemental material). Since recombinant REP_{pAL1} proteins fused to short affinity tags were present in the insoluble

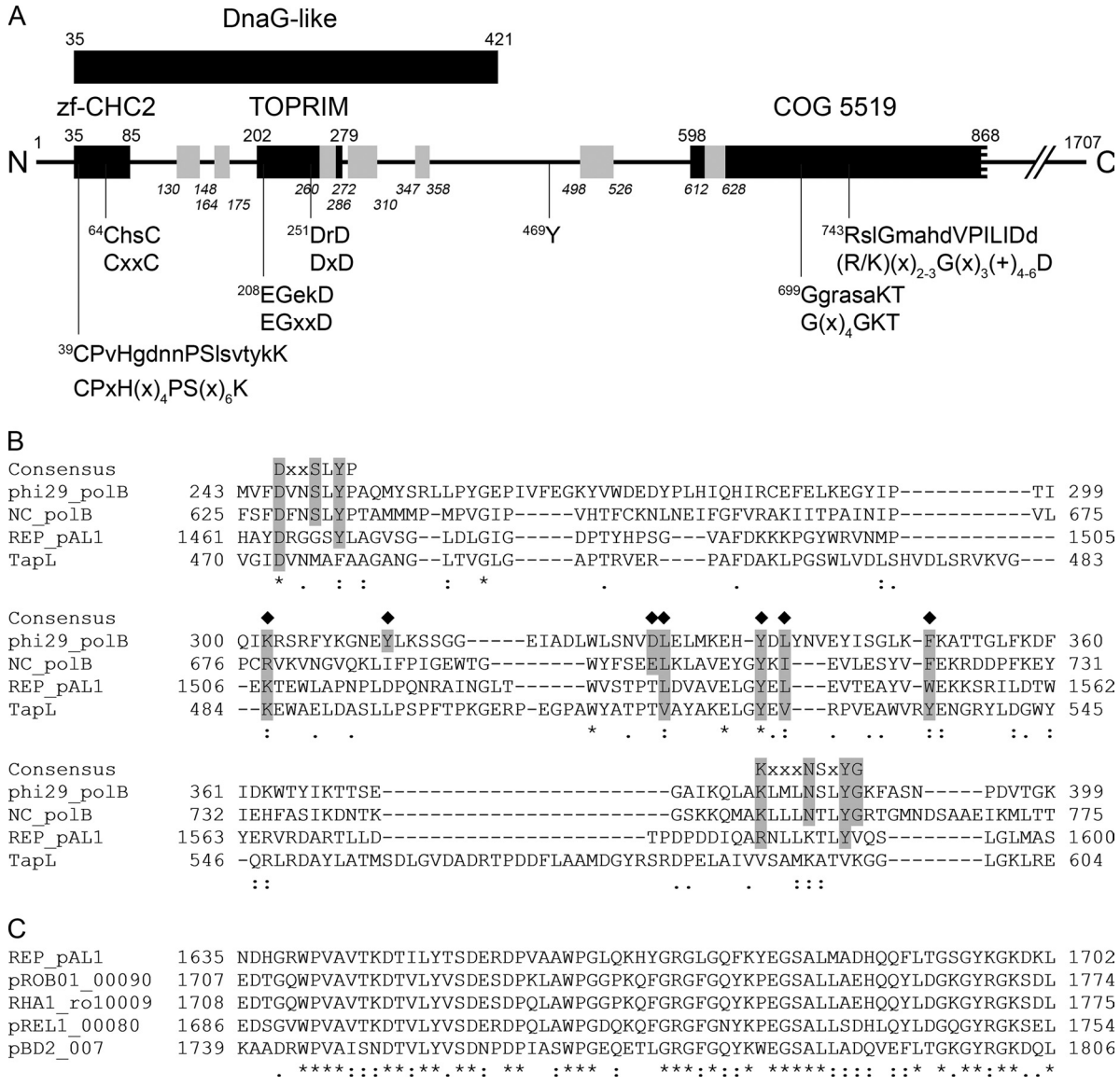

FIG. 1. Bioinformatic analysis of the REP_{pAL1} protein. (A) Hypothetical domain architecture and predicted sequence motifs of the N-terminal region of the REP_{pAL1} protein. The amino acid sequence of REP_{pAL1} (the gene product of *pAL1.101*; accession no. CAL09956) is represented by a line. The black bars, with residue numbers above each bar, indicate predicted conserved domains, namely, a DnaG-like domain (COG 0358; E value, 0.005), a CHC2 zinc finger subdomain (smart00400; E value, 0.001), and a Toprim subdomain (cd01029; E value, 3e-06), located within the DnaG region. A central region matched the N-terminal half of COG 5519, representing a superfamily II helicase and derivatives (E value, 3e-05). Searches for conserved domains against the CDD database were performed using the CD Search tool at NCBI (http://www.ncbi.nlm.nih.gov/Structure/cdd/wrpsb.cgi), with the low-complexity filter inactivated and an E value threshold of 0.01. Putative conserved amino acid motifs are indicated below the bars (x, any amino acid; +, hydrophobic amino acid); the lower lines indicate the consensus sequence of the respective motif (for references, see the text), and the associated upper lines show the amino acid sequence of REP_{pAL1}, with residues matching the consensus in uppercase. Residue Y469, which is conserved in rhodococcal homologs of REP_{pAL1}, is also indicated. The short bars in gray, with residue numbering in italics, correspond to tryptic peptides of REP_{pAL1} identified in the cross-linked TP_{pAL1}-REP_{pAL1} complex. For details, see the text. (B) Alignment of segments of phage ϕ29 DNA polymerase (phi29_polB; GenBank accession no. ACE96023), type B DNA polymerase of *Neurospora crassa* (NC_polB; CAA39046), REP_{pAL1} (REP_pAL1; CAL09956), and telomere-associated protein of *S. lividans* (TapL; AAO73842). The consensus sequence of motifs A and B of ϕ29 DNA polymerase, which is conserved among different nucleic-acid-synthesizing enzymes (7), is indicated above the sequences. Residues shaded in gray that are marked with a diamond above the sequence may represent conserved residues of the TPR-1 region, which is specific to protein-priming DNA polymerases (14, 15, 27, 37). (C) Alignment of a region rich in acidic residues, which is highly conserved among REP_{pAL1} (aa 1635 to 1702) and rhodococcal homologs. pROB01_00090 (BAH55508), putative telomere-binding protein of plasmid pROB01 of *R. opacus* B4; RHA1_ro10009 (ABH00202), possible transcriptional regulator of plasmid pRHL2 of *R. jostii* RHA1; pREL1_00080 (BAE45951), putative telomere-binding protein of plasmid pREL1 of *R. erythropolis* PR4; pBD2_007 (AAP73892), putative regulatory protein of plasmid pBD2 of *R. erythropolis* BD2. In panels B and C, residues conserved throughout are marked with asterisks, while residues marked with colons and dots are conserved and semiconserved substitutions, respectively.

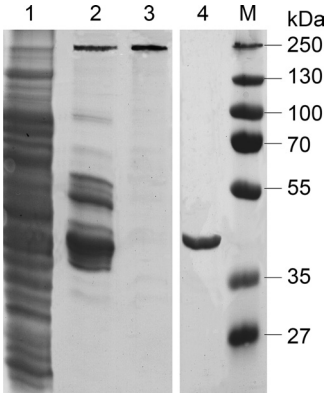

FIG. 2. Preparation of REP_{pAL1} fusion protein. Proteins from each preparation step were separated in a denaturing (SDS) polyacrylamide gel (10.8%; stained with ethyl violet/zincon). Lane 1, crude extract supernatant of *E. coli* Rosetta 2(DE3)(pLysSRARE2, pET22b-ORF101); lane 2, pool after amylose affinity chromatography containing the REP_{pAL1} fusion protein at 231 kDa and additional amylose binding proteins; lane 3, REP_{pAL1} fusion protein carrying an N-terminal MBP-His_7 and C-terminal His_6 tag after separation of the amylose pool by size exclusion chromatography (proteins of equivalent electrophoretic quality were used for all functional studies); lane 4, MBP-His_6 prepared from *E. coli* Rosetta 2(DE3)(pLysSRARE2, pET22b-malE-His_6), i.e., from the same genetic background as the REP_{pAL1} fusion protein, by amylose affinity chromatography; lane M, marker proteins.

fraction of the cell extract (data not shown), REP_{pAL1} was synthesized with an N-terminal fusion to MBP, which conferred *in vitro* solubility. The fusion protein (also termed REP_{pAL1}) was prepared by affinity chromatography, followed by size exclusion chromatography (Fig. 2). Since proteins from *E. coli* active on DNA might contaminate preparations of REP_{pAL1} (even if the protein appeared electrophoretically homogeneous), we prepared MBP-His_6 from *E. coli* Rosetta 2(DE3)(pLysSRARE2, pET22b-malE-His_6)—i.e., from an *E. coli* strain that, apart from the *pAL1.101* gene, is isogenic to the clone used for isolation of the REP_{pAL1} fusion protein—by the same amylose affinity chromatography protocol applied for the first step of REP_{pAL1} purification (Fig. 2, lane 4). This MBP-His_6 preparation should have contained the same (or rather, more) *E. coli* contaminants as the REP_{pAL1} preparations (which were subjected to a second chromatographic step after amylose affinity chromatography). MBP-His_6 was used as a control in all assays for catalytic functions of REP_{pAL1}.

DNA relaxation activity of REP_{pAL1}. The purified REP_{pAL1} fusion protein catalyzed the relaxation of negatively supercoiled circular DNA. The activity was ATP independent but required Mg^{2+} ions (Fig. 3A). Such a cofactor requirement, and the prediction of a Toprim domain (see above), may classify REP_{pAL1} as a type IA topoisomerase (47). In control experiments, treatment of plasmid DNA with topoisomerase I from calf thymus resulted in the formation of a DNA band with

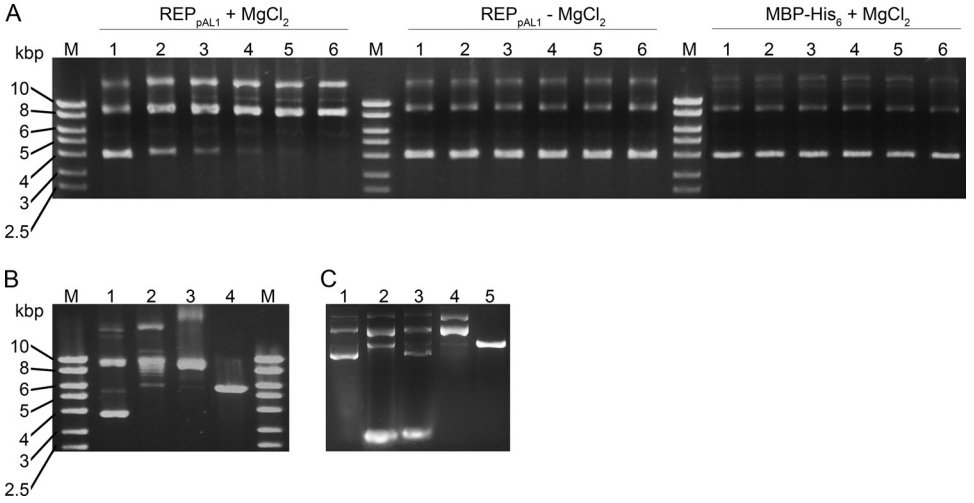

FIG. 3. Relaxation of supercoiled plasmid DNA by REP_{pAL1}. (A) Agarose gel (1%, ethidium bromide stained) of plasmid DNA treated with REP_{pAL1}. pET-22b(+) DNA (22.6 nM) was incubated at 30°C in 35 mM Tris-HCl, 72 mM KCl, 5 mM dithiothreitol (pH 8) with REP_{pAL1} (1.06 μM) in the presence and in the absence of 5 mM $MgCl_2$. Control assay mixtures contained 2.4 μM MBP-His_6 instead of REP_{pAL1}. Aliquots of the reaction mixtures were quenched by immersion in liquid nitrogen directly (time zero; lanes 1) and 20, 40, 60, 80, and 100 min (lanes 2 to 6) after the reaction was started. The prominent lower and middle bands represent supercoiled and relaxed circular DNA monomers, respectively (cf. panel B), whereas the upper band may represent relaxed dimers or multimers. Estimation of the supercoiled DNA in the samples treated with REP_{pAL1} plus $MgCl_2$, performed with the ImageJ program (v1.38j; open source; NIH, Bethesda, MD) after calibration with marker bands, indicated amounts of ~63 ng, 29 ng, 13 ng, 5 ng, 2 ng, and 1 ng in lanes 1, 2, 3, 4, 5, and 6, respectively. (B) Agarose gel (1%, ethidium bromide stained) of pET-22b(+) DNA. All assay mixtures contained 22.6 nM DNA. Lane 1, plasmid as isolated; lane 2, after treatment with DNA topoisomerase I from calf thymus (5 U, 37°C, 20 h); lane 3, after treatment with the site- and strand-specific endonuclease ("nickase") Nt.Bpu10I (1 U, 37°C, 2 h); lane 4, after linearization with restriction endonuclease HindIII (1 U, 37°C, 2 h). The same buffer (with 5 mM $MgCl_2$) as in panel A was used for all control experiments. The diffuse DNA band with low mobility in lane 3 may represent nicked multimers, DNA still associated with enzyme, or both. (C) DNA forms of pET-22b(+), separated in a 1% agarose gel containing 1 μg/ml ethidium bromide. The concentration of plasmid DNA in all assays was 22.6 nM. Lane 1, plasmid DNA as isolated; lane 2, after treatment with 1.06 μM REP_{pAL1} for 2 h at 37°C; lane 3, after incubation with an excess of DNA topoisomerase I from calf thymus (10 U, 37°C, 20 h); lane 4, after treatment with the nickase Nt.Bpu10I (1 U, 37°C, 2 h); lane 5, after linearization with HindIII (1 U, 37°C, 2 h). The same buffer (with 5 mM $MgCl_2$) as in panel A was used for all experiments. After incubation, the samples were supplemented with SDS (1%). Electrophoresis was performed at 2 V/cm for 15 min, paused for 5 min, and continued at 6 V/cm for 60 min.

mobility similar to that observed in the REP_{pAL1}-catalyzed reaction; under the conditions used, partially relaxed DNA was also visible (Fig. 3B, lane 2). However, nicked circular DNA, formed by the site-specific endonuclease Nt.Bpu10I, which is active on a single strand, showed electrophoretic mobility similar to that of the products of the topoisomerase reaction (Fig. 3B, lane 3). In order to distinguish between relaxed covalently closed circular DNA and nicked circular DNA, ethidium bromide was included in the agarose gel (Fig. 3C). Binding of the intercalating agent generates positive supercoiling in the covalently closed DNA, which significantly increases its electrophoretic mobility (11). Incubation of the plasmid DNA with an excess of topoisomerase I indeed yielded a DNA form which in the presence of ethidium bromide migrated very fast and thus is proposed to represent the covalently closed circular form (Fig. 3C, lane 3). Intercalators cannot overwind nicked DNA, which, irrespective of the presence of ethidium bromide, migrates above the linear form (Fig. 3C, lanes 4 and 5). The major DNA species formed in the REP_{pAL1}-catalyzed reaction (Fig. 3C, lane 2) showed the same fast electrophoretic mobility as the product of the topoisomerase reaction, suggesting that REP_{pAL1} exhibits topoisomerase activity.

DNA helicase activity of REP_{pAL1}. The capability of REP_{pAL1} to catalyze unwinding of double-stranded DNA was detected in a strand displacement assay, using oligomeric duplex DNA substrates consisting of a 5′-labeled and an unlabeled strand. REP_{pAL1} in the presence of ATP or dATP indeed mediated release of the labeled strand from the duplex DNA (Fig. 4A). Another assay, based on measuring liberation of the fluorescent dye DAPI from linearized dsDNA upon DNA unwinding, was performed with HindIII-linearized plasmid DNA as a substrate. Figure 4B shows kinetic traces of the unwinding of this linear dsDNA substrate at different concentrations of the REP_{pAL1} protein. Assuming that the fluorescence intensity of DAPI in the presence of the respective dsDNA and in the presence of the heat-denatured DNA substrate represented 0% and 100% unwinding of DNA, respectively, the estimated initial rate of REP_{pAL1}-catalyzed unwinding of dsDNA was in the range of 10^5 bp/s per enzyme monomer. Unwinding of 5′-biotinylated fully complementary dsDNA, which was tested as a model for 5′-capped linear dsDNA, occurred at a similar apparent initial rate. Such estimated unwinding rates are higher than those reported for other DNA helicases. The RecBCD enzyme, for example, showed a maximum rate of between 1,000 and 1,500 bp/s (4, 12). However, since several replicative DNA helicases have been described as much more effective when complexed with the polymerase or with accessory proteins of the replisome (13, 28, 55), it is tempting to speculate that the high apparent unwinding rate of REP_{pAL1} *in vitro* might be due to the presence of modulating domains on the same polypeptide.

Many DNA helicases require a single-stranded tail as a loading site (31, 46), whereas REP_{pAL1} appears to also be active toward blunt-ended, 5′-capped dsDNA. Such activity is consistent with a possible role in initiating replication of linear plasmid DNA from its telomeres.

Template-specific deoxycytidylation of TP_{pAL1} by REP_{pAL1} and TP_{pAL1}- and DNA-primed polymerase activity. To investigate whether TP_{pAL1} can act as a priming protein for DNA replication, we previously developed an *in vitro* deoxynucleotidylation assay that contained the ssDNA template left70 (see Table S2 in the supplemental material), representing the 3′-terminal 70 nucleotides of the "left" end of pAL1; MBP-TP_{pAL1}; crude extract of *A. nitroguajacolicus* Rü61a; the REP_{pAL1} fusion protein; ATP; and different [α-^{32}P]dNTPs in Mg^{2+}-containing buffer. Specific deoxycytidylation of TP_{pAL1} was detected in the presence of the ssDNA template, tentatively suggesting that the terminal or subterminal guanosine nucleotide at the 3′ end of pAL1 might serve as a template for the nucleotide incorporation reaction (30). When the *Arthrobacter* cell extract in the assay was replaced by bovine serum albumin (BSA), incorporation of [^{32}P]dCMP into TP_{pAL1} occurred at similar intensity (Fig. 5A, compare lanes left70 + BSA and left70), indicating that REP_{pAL1} is sufficient to catalyze the reaction.

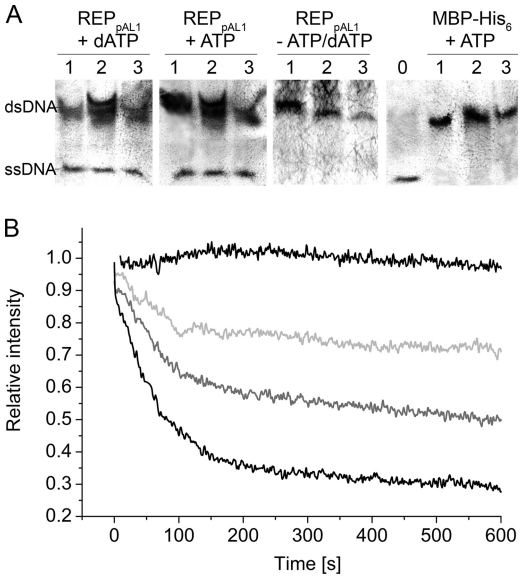

FIG. 4. DNA helicase activity of REP_{pAL1}. (A) Immunodetection of DIG-labeled DNA oligomers after separation in a 15% polyacrylamide gel and Southern blotting. REP_{pAL1} catalyzed the displacement of DIG-labeled ssDNA from oligomeric DNA duplex substrates consisting of the 5′-DIG-labeled oligomer DIG29basic and complementary unlabeled strands. The duplex DNA substrates had 6-nucleotide 3′ overhangs (DIG29basic plus 29-3; lanes 1), 6-nucleotide 5′ overhangs (DIG29basic plus 29-5; lanes 2), and blunt ends (DIG29basic plus blunt29; lanes 3). For oligonucleotide sequences, see Table S2 in the supplemental material. The assays contained 10 nM duplex DNA substrate, a 100-fold excess of unlabeled competitor ssDNA, 2 mM ATP or dATP, and 0.14 μM REP_{pAL1} or 10 μM MBP-His_6 (as the negative control) in 35 mM Tris-HCl, 72 mM KCl, 5 mM dithiothreitol, 5 mM $MgCl_2$ (pH 8). All assay mixtures were incubated for 2 h at 30°C. The lane marked 0 shows the electrophoretic mobility of the 5′-DIG-labeled single-stranded 29-mer DIG29basic. (B) Fluorescence quenching upon unwinding of dsDNA as a function of the REP_{pAL1} concentration. The kinetic traces of fluorescence decrease are shown for assays containing 2 pM of MBP-His_6 instead of REP_{pAL1} (control; upper black line) and 0.5 pM (light gray), 1 pM (dark gray), and 2 pM (lower black line) of REP_{pAL1} fusion protein. The dsDNA substrate (HindIII-linearized pUC18 DNA; 1 nM), DAPI (4 μM), and 5 mM ATP in 35 mM Tris-HCl, 72 mM KCl, 5 mM dithiothreitol, 5 mM $MgCl_2$ (pH 8) was equilibrated for 1 h in the dark before the reaction was started by the addition of REP_{pAL1} protein. The DAPI fluorescences of dsDNA and ssDNA substrates were defined as relative intensities 1 and 0, respectively.

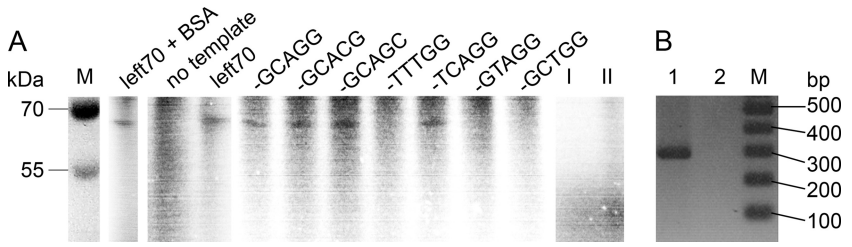

FIG. 5. Template specificity of REP_{pAL1}-catalyzed deoxycytidylation of TP_{pAL1} (A) and TP_{pAL1}-primed amplification of dsDNA (B). (A) Deoxynucleotidylation assay mixtures contained 1.0 μM purified MBP-TP_{pAL1} protein, 0.1 μM REP_{pAL1} fusion protein, 1 mM ATP, 1 μM DNA template, [α-^{32}P]dCTP (0.33 μM; 111 TBq/mmol; PerkinElmer, Rodgau-Jügesheim, Germany), and either 0.05 mg/ml BSA (lane left70 + BSA) or crude extract (soluble proteins) of *A. nitroguajacolicus* Rü61a(pAL1) (0.33 mg protein/ml; all other lanes) in 35 mM Tris-HCl, 72 mM KCl, 5 mM dithiothreitol, 5 mM $MgCl_2$ (pH 8). The samples were incubated for 16 h at 30°C. After treatment with 10 U DNase I at 30°C for 1 h, samples were separated in a 10% SDS-polyacrylamide gel, and radiolabeled proteins were detected with a phosphorimager (PharosFX Plus; Bio-Rad Laboratories). The template left70 represents the 3′-terminal 70 nucleotides of the left end of pAL1 with the terminal sequence GCAGG-3′, which is conserved at both 3′ ends of pAL1. Other templates (20-mer ssDNA) (see Table S2 in the supplemental material) showed variations of the 3′-terminal sequence, as indicated above the lanes. In lanes I and II, MBP-TP_{pAL1} and REP_{pAL1}, respectively, were replaced by equimolar concentrations of MBP-His_6 protein; the control assays contained left70 DNA template. (B) Lane 1, dsDNA (285-bp l285 [see Table S2 in the supplemental material]; 0.3 μM), MBP-TP_{pAL1} (65 nM) as a protein primer, ATP (2 mM), and dNTPs (200 μM each) were incubated with REP_{pAL1} fusion protein (0.1 μM) at 30°C in 35 mM Tris-HCl, 72 mM KCl, 5 mM dithiothreitol, 5 mM $MgCl_2$ (pH 8) for 24 h. A control assay was performed in the same way, except that REP_{pAL1} was replaced by MBP-His_6 protein (lane 2). Samples were treated with 0.5 mg/ml proteinase K prior to electrophoresis in a 2% agarose gel (ethidium bromide stain). Estimation of the amount of DNA in the 285-bp band, performed with the ImageJ program (v1.38j; open source; NIH, Bethesda, MD) after calibration with marker bands, indicated about 51 ng dsDNA in lane 1.

Deoxycytidylation of TP_{pAL1} at both the left70 template and the 20-mer 5′-CAGTTCGCATCTATTGCAGG-3′—which, aside from the terminal inverted-repeat sequence GCAGG-3′, consists of random nucleotides—suggests that distal regions of the 3′ end are not essential for the reaction (Fig. 5A, lane -GCAGG). To address the requirement for a conserved terminal sequence, the 3′ end of the 20-mer was varied. The REP_{pAL1}-catalyzed deoxycytidylation of TP_{pAL1} required conservation of the third and fourth nucleotides (CA) of the template sequence, whereas a G→T transversion of the distal nucleotide of the 3′-terminal inverted-repeat sequence did not interfere with the reaction. Surprisingly, incorporation of dCMP into TP_{pAL1} occurred at several templates having GG-3′, GC-3′, and CG-3′ ends, suggesting that under the assay conditions used, deoxycytidylation of TP_{pAL1} by REP_{pAL1} does not show strict preference for the 3′-terminal or the subterminal guanosine nucleotide of the template (Fig. 5A). In the case of subterminal initiation, replication at the pAL1 telomere *in vivo* should involve a "sliding-back" mechanism, as shown for protein-primed replication of phage genomes, to maintain the integrity of the DNA ends (25, 32, 33). Subterminal initiation followed by "sliding back" for transition from protein-primed initiation to DNA elongation was proposed to be a general feature of protein-primed replication systems (7, 33).

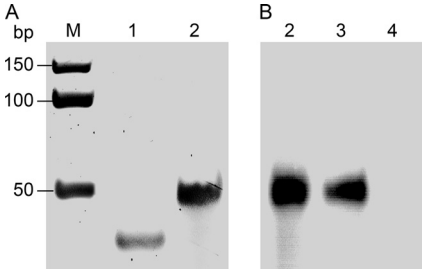

FIG. 6. DNA primer elongation by REP_{pAL1}. Shown are a polyacrylamide gel (15%; ethidium bromide stained) (A) and an autoradiograph of the polyacrylamide gel (B), both detected with a phosphorimager (PharosFX Plus; Bio-Rad Laboratories). Lane 1 shows the DNA substrate, i.e., the 13-mer primer (left13t) hybridized to the 50-mer template (left50). For oligonucleotide sequences, see Table S2 in the supplemental material. Elongation assay mixtures contained the unlabeled DNA hybrid left50/left13t (1 μM) (lane 1); 66 nM (each) dATP, dGTP, dTTP, and [α-^{32}P]-dCTP; and either GoTaq DNA polymerase (A and B, lanes 2), REP_{pAL1} fusion protein (88 nM) (B, lane 3), or MBP-His_6 protein (800 nM) (lane 4) in 35 mM Tris-HCl, 72 mM KCl, 5 mM dithiothreitol, 5 mM $MgCl_2$ (pH 8). The GoTaq-catalyzed elongation reaction shown in the ethidium bromide-stained gel (A, lane 2) was performed with 5 U of DNA polymerase, whereas for the autoradiographic detection (B, lane 2), only 0.1 U of GoTaq DNA polymerase was used in the assay, in order to achieve a signal intensity similar to that of the REP_{pAL1}-catalyzed elongation reaction (lane 3). The assay mixtures were incubated for 1 h at 22°C. Lane M, dsDNA marker.

Isothermal amplification of a 285-bp dsDNA template using TP_{pAL1} as a protein primer resulted in production of a distinct, full-length amplification product (Fig. 5B), suggesting that REP_{pAL1} can act as a combined helicase and protein-primed DNA polymerase. To determine whether REP_{pAL1} also catalyzes DNA-primed elongation reactions, a primer extension assay was carried out using a 13-nucleotide DNA primer hybridized to a 50-mer DNA template. As shown in Fig. 6, lane 3, the primer was extended up to the full length of the template, resulting in a 50-bp dsDNA product.

DISCUSSION

With a combination of DNA topoisomerase, DNA helicase, and protein-primed, as well as DNA-primed, DNA polymerase activities, REP_{pAL1} is a novel type of replicative enzyme. It is obvious that more detailed biochemical studies must be performed to quantitatively characterize its function. Nevertheless, the present data show that the protein in principle provides all the catalytic activities necessary for protein-primed synthesis of ssDNA at a parental duplex DNA. However, template-dependent REP_{pAL1}-catalyzed deoxynucleotidylation of

TP_{pAL1}, as well as amplification of dsDNA with TP_{pAL1} as a primer, required very long incubation times (Fig. 5), suggesting that the protein-priming step proceeded very inefficiently. Moreover, our attempts to amplify long (several-kbp) DNA templates, using REP_{pAL1} as the only replicative enzyme and either TP_{pAL1} or DNA oligomers as the primer, have failed (data not shown), indicating low processivity of the DNA polymerase under the conditions used. Even though we cannot exclude the possibility that the MBP tags fused to both TP_{pAL1} and REP_{pAL1} impede the deoxynucleotidylation and polymerization steps, it is conceivable that in the *in vivo* situation, accessory protein factors contribute to efficient protein priming and improve the processivity of the DNA polymerase. Accessory proteins are common components of bacterial replisomes and of replicative complexes of phage genomes (21). Remarkably, *in vitro* replication of full-length (19,285-bp) TP-linked ϕ29 DNA by the strand displacement mechanism could be accomplished with only the presence of TP and ϕ29 DNA polymerase (5), but highly efficient DNA amplification also required the dsDNA-binding phage protein p6, which recognizes the ϕ29 DNA ends and forms a nucleoprotein complex, and the ssDNA-binding (SSB) protein p5 (6). Protein-protein- and protein-DNA interaction studies will be required to identify all the components of a possible replicative protein complex on pAL1.

Another key question concerns the mode of replication of pAL1 *in vivo*. REP_{pAL1}, presumably in complex with accessory proteins, might catalyze protein-primed replication of full-length pAL1-DNA initiated at the telomeres. Alternatively, if replication of pAL1 is initiated from an internal origin, REP_{pAL1} might be part of a telomere complex that binds to 3′ overhangs of replication intermediates, unwinds secondary structures of the overhangs, and fills in the recessed 5′ ends.

The DNA region representing an origin of replication may be predicted by analysis of the DNA strand compositional asymmetry. In most bidirectionally replicated genomes, origins of replication are represented by a minimum in the cumulative GC skew diagram (18). For pAL1, the cumulative GC skew plot exhibits three local minima at about 32 kbp, 58 to 61 kbp, and 73 kbp; however, the global minimum actually localizes at the "right" end of pAL1 (see Fig. S1 in the supplemental material).

In a number of studies on actinomycetal linear plasmids, their replication regions containing the internal origin were identified by cloning DNA fragments of the linear plasmid into a vector that was unable to replicate in actinomycetes. Inserts comprising the replication region conferred on the recombinant plasmid the ability to replicate autonomously in circular form in the actinomycete (for examples, see references 23, 38, and 57). In an analogous approach, we inserted fragments of pAL1 into a pUC18-based vector containing the *cmx* gene, encoding a chloramphenicol efflux protein, as a selectable marker. Restriction fragments of total pAL1 DNA, as well as PCR-generated fragments in sizes of 5 to 10 kbp, which cover overlapping internal parts of pAL1, including the regions which in the cumulative GC-skew diagram shows local minima, were used to generate plasmid libraries. However, transformation of a pAL1-deficient mutant of *A. nitroguajacolicus* Rü61a failed to yield plasmid-containing clones; the occasional chloramphenicol-resistant transformants all contained ectopic insertions of plasmid DNA into the genome (data not shown). Since our present attempts to isolate an internal region required for replication failed, either the relevant fragment was not part of the libraries tested or loci necessary for replication are dispersed on pAL1. Alternatively, replication of pAL1 might indeed be initiated at the telomere. More detailed studies will be required to elucidate the mode of replication of the linear *Arthrobacter* plasmid pAL1.

ACKNOWLEDGMENTS

We thank R. Brandsch (University of Freiburg, Freiburg, Germany) for kindly providing the vector pART2, A. Steinbüchel (Münster, Germany) for access to the phosphorimager, Katja Parschat and Heiko Niewerth for construction of pART2-ORF102, and Katja Parschat for experiments aimed at the identification of the replication region of pAL1 and for discussions and helpful comments on the manuscript. We also thank Almut Kappius for excellent technical assistance.

This work was supported by grants FE 383/11-1 and 11-2 from the Deutsche Forschungsgemeinschaft (DFG) to S.F. and by a 6-month research grant from the University of Münster to S.K.

REFERENCES

1. **Aravind, L., D. D. Leipe, and E. V. Koonin.** 1998. Toprim: a conserved catalytic domain in type IA and II topoisomerases, DnaG-type primases, OLD family nucleases and RecR proteins. Nucleic Acids Res. **26:**4205–4213.
2. **Bao, K., and S. N. Cohen.** 2001. Terminal proteins essential for the replication of linear plasmids and chromosomes in *Streptomyces*. Genes Dev. **15:**1518–1527.
3. **Bao, K., and S. N. Cohen.** 2003. Recruitment of terminal protein to the ends of *Streptomyces* linear plasmids and chromosomes by a novel telomere-binding protein essential for linear DNA replication. Genes Dev. **17:**774–785.
4. **Bianco, P. R., L. R. Brewer, M. Corzett, R. Balhorn, Y. Yeh, S. C. Kowalczykowski, and R. J. Baskin.** 2001. Processive translocation and DNA unwinding by individual RecBCD enzyme molecules. Nature **409:**374–378.
5. **Blanco, L., A. Bernad, J. M. Lázaro, G. Martín, C. Garmendia, and M. Salas.** 1989. Highly efficient DNA synthesis by the phage ϕ29 DNA polymerase. Symmetrical mode of DNA replication. J. Biol. Chem. **264:**8935–8940.
6. **Blanco, L., J. M. Lázaro, M. De Vega, A. Bonnin, and M. Salas.** 1994. Terminal protein-primed DNA amplification. Proc. Natl. Acad. Sci. U. S. A. **91:**12198–12202.
7. **Blanco, L., and M. Salas.** 1996. Relating structure to function in ϕ29 DNA polymerase. J. Biol. Chem. **271:**8509–8512.
8. **Caruthers, J. M., and D. B. McKay.** 2002. Helicase structure and mechanism. Curr. Opin. Struct. Biol. **12:**123–133.
9. **Chang, P.-C., and S. N. Cohen.** 1994. Bidirectional replication from an internal origin in a linear *Streptomyces* plasmid. Science **265:**952–954.
10. **Choi, J. K., K. H. Tak, L. T. Jin, S. Y. Hwang, T. I. Kwon, and G. S. Yoo.** 2002. Background-free fast protein staining in sodium dodecyl sulfate polyacrylamide gel using counterion dyes, zincon and ethyl violet. Electrophoresis **23:**4053–4059.
11. **Dexheimer, T. S., and Y. Pommier.** 2008. DNA cleavage assay for the identification of topoisomerase I inhibitors. Nat. Protoc. **3:**1736–1750.
12. **Dillingham, M. S., M. R. Webb, and S. C. Kowalczykowski.** 2005. Bipolar DNA translocation contributes to highly processive DNA unwinding by RecBCD enzyme. J. Biol. Chem. **280:**37069–37077.
13. **Dong, F., S. E. Weitzel, and P. H. von Hippel.** 1996. A coupled complex of T4 DNA replication helicase (gp41) and polymerase (gp43) can perform rapid and processive DNA strand-displacement synthesis. Proc. Natl. Acad. Sci. U. S. A. **93:**14445–14461.
14. **Dufour, E., J. Méndez, J. M. Lázaro, M. de Vega, L. Blanco, and M. Salas.** 2000. An aspartic acid residue in TPR-1, a specific region of protein-priming DNA polymerases, is required for the functional interaction with primer terminal protein. J. Biol. Chem. **304:**289–300.
15. **Dufour, E., I. Rodríguez, J. M. Lázaro, M. de Vega, and M. Salas.** 2003. A conserved insertion in protein-primed DNA polymerases is involved in primer terminus stabilisation. J. Mol. Biol. **331:**781–794.
16. **Eggleston, A. K., N. A. Rahim, and S. C. Kowalczykowski.** 1996. A helicase assay based on the displacement of fluorescent, nucleic-acid binding ligands. Nucleic Acids Res. **24:**1179–1186.
17. **Gartemann, K. H., and R. Eichenlaub.** 2001. Isolation and characterization of IS1409, an insertion element of 4-chlorobenzoate-degrading *Arthrobacter* sp. strain TM1, and development of a system for transposon mutagenesis. J. Bacteriol. **183:**3729–3736.
18. **Grigoriev, A.** 1998. Analyzing genomes with cumulative skew diagrams. Nucleic Acids Res. **26:**2286–2290.

19. **Grishin, N. V.** 2000. C-terminal domains of *Escherichia coli* topoisomerase I belong to the zinc-ribbon superfamily. J. Mol. Biol. **299:**1165–1177.
20. **Hall, M. C., and S. W. Matson.** 1999. Helicase motifs: the engine that powers DNA unwinding. Mol. Microbiol. **34:**867–877.
21. **Hamdan, S. M., and C. C. Richardson.** 2009. Motors, switches, and contacts in the replisome. Annu. Rev. Biochem. **78:**205–243.
22. **Hanahan, D.** 1983. Studies on transformation of *Escherichia coli* with plasmids. J. Mol. Biol. **166:**557–580.
23. **Hiratsu, K., S. Mochizuki, and H. Kinashi.** 2000. Cloning and analysis of the replication origin and the telomeres of the large linear plasmid pSLA2-L in *Streptomyces rochei*. Mol. Gen. Genet. **263:**1015–1021.
24. **Huang, C.-H., H.-H. Tsai, Y.-G. Tsay, Y.-N. Chien, S.-L. Wang, M.-Y. Cheng, C.-H. Ke, and C. W. Chen.** 2007. The telomere system of the *Streptomyces* linear plasmid SCP1 represents a novel class. Mol. Microbiol. **63:**1710–1718.
25. **Illana, B., L. Blanco, and M. Salas.** 1996. Functional characterization of the genes coding for the terminal protein and DNA polymerase from bacteriophage GA-1. Evidence for a sliding-back mechanism during protein-primed GA-1 DNA replication. J. Mol. Biol. **264:**453–464.
26. **Kamtekar, S., A. J. Berman, J. Wang, J. M. Lázaro, M. de Vega, L. Blanco, M. Salas, and T. A. Steitz.** 2004. Insights into strand displacement and processivity from the crystal structure of the protein-primed DNA polymerase of bacteriophage ϕ29. Mol. Cell **16:**609–618.
27. **Kamtekar, S., J. Méndez, J. M. Lázaro, M. de Vega, L. Blanco, and M. Salas.** 2006. The ϕ29 DNA polymerase:protein-primer structure suggests a model for the initiation to elongation transition. EMBO J. **25:**1335–1343.
28. **Kim, S., H. G. Dallmann, C. S. McHenry, and K. J. Marians.** 1996. Coupling of a replicative polymerase and helicase: a τ-DnaB interaction mediates rapid replication fork movement. Cell **84:**643–650.
29. **Klassen, R., and F. Meinhardt.** 2007. Linear protein-primed replicating plasmids in eukaryotic microbes, p. 187–226. *In* F. Meinhardt and R. Klassen (ed.), Microbial linear plasmids. Microbiology monograph 7. Springer, Heidelberg, Germany.
30. **Kolkenbrock, S., and S. Fetzner.** 2010. Identification and *in vitro* deoxynucleotidylation of the terminal protein of the linear plasmid pAL1 of *Arthrobacter nitroguajacolicus* Rü61a. FEMS Microbiol. Lett. **304:**169–176.
31. **Lohman, T. M., and K. P. Bjornson.** 1996. Mechanisms of helicase-catalyzed DNA unwinding. Annu. Rev. Biochem. **65:**169–214.
32. **Martín, A. C., L. Blanco, P. García, and M. Salas.** 1996. *In vitro* initiation of pneumococcal phage Cp-1 DNA replication occurs at the third 3′ nucleotide of the linear template: a stepwise sliding-back mechanism. J. Mol. Biol. **260:**369–377.
33. **Méndez, J., L. Blanco, J. A. Esteban, A. Bernad, and M. Salas.** 1992. Initiation of ϕ29 DNA replication occurs at the second 3′-nucleotide of the linear template: a sliding-back mechanism for protein-primed DNA replication. Proc. Natl. Acad. Sci. U. S. A. **89:**9579–9583.
34. **Overhage, J., S. Sielker, S. Homburg, K. Parschat, and S. Fetzner.** 2005. Identification of large linear plasmids in *Arthrobacter* spp. encoding the degradation of quinaldine to anthranilate. Microbiology **151:**491–500.
35. **Parschat, K., B. Hauer, R. Kappl, R. Kraft, J. Hüttermann, and S. Fetzner.** 2003. Gene cluster of *Arthrobacter ilicis* Rü61a involved in the degradation of quinaldine to anthranilate. J. Biol. Chem. **278:**27483–27494.
36. **Parschat, K., J. Overhage, A. W. Strittmatter, A. Henne, G. Gottschalk, and S. Fetzner.** 2007. Complete nucleotide sequence of the 113-kilobase linear catabolic plasmid pAL1 of *Arthrobacter nitroguajacolicus* Rü61a and transcriptional analysis of genes involved in quinaldine degradation. J. Bacteriol. **189:**3855–3867.
37. **Pérez-Arnaiz, P., E. Longás, L. Villar, J. M. Lázaro, M. Salas, and M. de Vega.** 2007. Involvement of phage ϕ29 DNA polymerase and terminal protein subdomains in conferring specificity during initiation of protein-primed DNA replication. Nucleic Acids Res. **35:**7061–7073.
38. **Picardeau, M., C. Le Dantec, and V. Vincent.** 2000. Analysis of the internal replication region of a mycobacterial linear plasmid. Microbiology **146:**305–313.
39. **Rainey, F. A., N. Ward-Rainey, R. M. Kroppenstedt, and E. Stackebrandt.** 1996. The genus *Nocardiopsis* represents a phylogenetically coherent taxon and a distinct actinomycete lineage: proposal of *Nocardiopsaceae* fam. nov. Int. J. Syst. Bacteriol. **46:**1088–1092.
40. **Roche Molecular Biochemicals.** 1995. The DIG system user's guide for filter hybridization. Boehringer Mannheim GmbH, Mannheim, Germany.
41. **Roman, L. J., and S. C. Kowalczykowski.** 1989. Characterization of the helicase activity of the *Escherichia coli* RecBCD enzyme using a novel helicase assay. Biochemistry **28:**2863–2873.
42. **Salas, M.** 1991. Protein-priming of DNA replication. Annu. Rev. Biochem. **60:**39–71.
43. **Salas, M., L. Blanco, J. M. Lázaro, and M. de Vega.** 2008. The bacteriophage ϕ29 DNA polymerase. IUBMB Life **60:**82–85.
44. **Salas, M., R. Freire, M. S. Soengas, J. A. Esteban, J. Méndez, A. Bravo, M. Serrano, M. A. Blasco, J. M. Lázaro, L. Blanco, C. Gutiérrez, and J. M. Hermoso.** 1995. Protein-nucleic acid interactions in bacteriophage ϕ29 DNA replication. FEMS Microbiol. Rev. **17:**73–82.
45. **Sambrook, J., and D. W. Russell.** 2001. Molecular cloning: a laboratory manual. Cold Spring Harbor Laboratory, Cold Spring Harbor, NY.
46. **Singleton, M. R., and D. B. Wigley.** 2002. Modularity and specialization in superfamily 1 and 2 helicases. J. Bacteriol. **184:**1819–1826.
47. **Sissi, C., and M. Palumbo.** 2009. Effects of magnesium and related divalent metal ions in topoisomerase structure and function. Nucleic Acids Res. **37:**702–711.
48. **Smith, P. K., R. I. Krohn, G. T. Hermanson, A. K. Mallia, F. H. Gartner, M. D. Provenzano, E. K. Fujimoto, N. M. Goeke, B. J. Olson, and D. C. Klenk.** 1985. Measurement of protein using bicinchoninic acid. Anal. Biochem. **150:**76–85.
49. **Stauber, E. J., A. Busch, B. Naumann, A. Svatos, and M. Hippler.** 2009. Proteotypic profiling of LHCI from *Chlamydomonas reinhardtii* provides new insights into structure and function of the complex. Proteomics **9:**398–408.
50. **Stauber, E. J., A. Fink, C. Markert, O. Kruse, U. Johanningmeier, and M. Hippler.** 2003. Proteomics of *Chlamydomonas reinhardtii* light-harvesting proteins. Eukaryot. Cell **2:**978–994.
51. **Steitz, T. A.** 1999. DNA polymerases: structural diversity and common mechanisms. J. Biol. Chem. **274:**17395–17398.
52. **Stoll, A., M. Redenbach, and J. Cullum.** 2007. Identification of essential genes for linear replication of an SCP1 composite plasmid. FEMS Microbiol. Lett. **270:**146–154.
53. **Studier, F. W.** 2005. Protein production by auto-induction in high-density shaking cultures. Protein Expr. Purif. **41:**207–234.
54. **Suzuki, H., K. Marushima, Y. Ohnishi, and S. Horinouchi.** 2008. A novel pair of terminal protein and telomere-associated protein for replication of the linear chromosome of *Streptomyces griseus* IFO13350. Biosci. Biotechnol. Biochem. **72:**2973–2980.
55. **Trego, K. S., and D. S. Parris.** 2003. Functional interaction between the herpes simplex virus type 1 polymerase processivity factor and origin-binding proteins: Enhancement of UL9 helicase activity. J. Virol. **77:**12646–12659.
56. **Walker, J. E., M. Saraste, M. J. Runswick, and N. J. Gay.** 1982. Distantly related sequences in the α- and β-subunits of ATP synthase, myosin, kinases and other ATP-requiring enzymes and a common nucleotide binding fold. EMBO J. **1:**945–951.
57. **Warren, R., W. W. L. Hsiao, H. Kudo, M. Myhre, M. Dosanjh, A. Petrescu, H. Kobayashi, S. Shimizu, K. Miyauchi, E. Masai, G. Yang, J. M. Stott, J. E. Schein, H. Shin, J. Khattra, D. Smailus, Y. S. Butterfield, A. Siddiqui, R. Holt, M. A. Marra, S. J. M. Jones, W. W. Mohn, F. S. L. Brinkman, M. Fukuda, J. Davies, and L. D. Eltis.** 2004. Functional characterization of a catabolic plasmid from polychlorinated-biphenyl-degrading *Rhodococcus* sp. strain RHA1. J. Bacteriol. **186:**7783–7795.
58. **Yang, C.-C., Y.-H. Chen, H.-H. Tsai, C.-H. Huang, T.-W. Huang, and C. W. Chen.** 2006. In vitro deoxynucleotidylation of the terminal protein of *Streptomyces* linear chromosomes. Appl. Environ. Microbiol. **72:**7959–7961.
59. **Zhang, R., Y. Yang, P. Fang, C. Jiang, L. Xu, Y. Zhu, M. Shen, H. Xia, J. Zhao, T. Chen, and Z. Qin.** 2006. Diversity of telomere palindromic sequences and replication genes among *Streptomyces* linear plasmids. Appl. Environ. Microbiol. **72:**5728–5733.
60. **Zhang, R., H. Xia, P. Guo, and Z. Qin.** 2009. Variation in the replication loci of *Streptomyces* linear plasmids. FEMS Microbiol. Lett. **290:**209–216.